Vitrectomy for Diabetic Macular Edema: Optical Coherence Tomography Criteria and Pathology of the Vitreomacular Interface

FELIX HAGENAU, DENISE VOGT, JEAN ZIADA, STEFANIE R. GUENTHER, CHRISTOS HARITOGLOU, ARMIN WOLF, SIEGFRIED G. PRIGLINGER, AND RICARDA G. SCHUMANN

• PURPOSE: To correlate spectral-domain optical coherence tomography (SDOCT) criteria and clinical data with pathology of the vitreomacular interface (VMI) in eyes with diabetic macular edema (DME).

• DESIGN: Retrospective cross-sectional study and laboratory investigation.

• METHODS: We included specimens of 27 eyes of 26 patients with center-involved DME that underwent vitrectomy with peeling of the internal limiting membrane (ILM). Selection of specimens was consecutive and in retrospect using our register of the Vitreoretinal Pathology Unit. Clinical data and SDOCT examinations were correlated to immunocytochemistry and transmission electron microscopy. Classification of DME comprised sponge-like diffuse retinal thickening, cystoid macular edema, and serous retinal detachment. VMI was evaluated for presence of epiretinal membrane (ERM) and thickened vitreous cortex (tVC).

• RESULTS: ERMs and tVC were found in all DME types. Diffuse DME showed tVC more often than cystoid DME. Hyalocytes, contractile myofibroblasts, glial cells, matrix metalloproteinases-2 and -9, and collagen type I, II, and III were positive tested irrespective of DME type. There were no significant cell fragments at the retinal side of the ILM. Visual acuity improved in the majority of cases and macular thickness decreased significantly during mean follow-up of 17 ± 10 months.

• CONCLUSIONS: All eyes presented pathologic VMI changes irrespective of the OCT classification of DME type or presence of ERM. Composition of fibrocellular membranes at the VMI indicated remodeling of vitreous cortex and transdifferentiation of hyalocytes into myofibroblasts. Our findings might argue for an early surgical intervention in eyes with DME irrespective of the presence of traction formation imaged by SDOCT. (Am J Ophthalmol 2019;200:34–46. © 2018 Elsevier Inc. All rights reserved.)

Accepted for publication Dec 4, 2018.

From the Department of Ophthalmology, Ludwig-Maximilians-University, Munich, Germany (F.H., D.V., J.Z., S.R.G., A.W., S.G.P., R.G.S.); and Duke Carl Theodor Eye Clinic, Munich, Germany (C.H.).

Inquiries to Felix Hagenau, Department of Ophthalmology, Ludwig-Maximilians-University, Mathildenstrasse 8, 80336 Munich, Germany; e-mail: fhagenau@med.lmu.de

DIABETIC MACULAR EDEMA (DME) OCCURS IN MORE than 7% of patients with diabetic retinopathy and represents the main cause of progressive vision loss during the course of disease.[1] Despite recent advantages in the management of DME, therapy remains challenging in many cases.

To date, first-line treatment of center-involved DME consists of pharmacotherapy with intravitreal injections of anti–vascular endothelial growth factor (anti-VEGF) agents or steroids,[2–7] thereby counteracting 2 major pathogenetic factors, namely blood–retina barrier breakdown and inflammation.[8,9] Other factors were also shown to play a role in the development and progression of DME, such as alterations of the vitreous and the vitreomacular interface (VMI) with epiretinal membrane (ERM) formation and internal limiting membrane (ILM) thickening.[10–13] These changes were addressed by pars plana vitrectomy (PPV) with or without ILM peeling in the past. At times when intravitreal pharmacotherapy had not been available, PPV and laser photocoagulation were the most important therapeutic players in the DME treatment regimen.[14]

Consistent with the guidelines for the management of DME by retina specialists, PPV is currently recommended as a therapeutic option in cases of DME associated with tractional changes at the VMI.[2] In the absence of traction formation, there is no consensus on the role of PPV in the actual treatment algorithm of diabetic eyes. However, it was previously shown that the rate of molecular transport can be increased not only by a physiological reduction of viscosity (liquefaction) and vitreous detachment with age[15] but also by other means, including vitrectomy.[16] This effect may therefore be beneficial in ischemic retinal disease, resulting in a decrease of the VEGF concentration at the retinal surface and an increase of the oxygen supply in ischemic areas, respectively.[16] Oxygen has been shown to suppress VEGF gene expression and therefore is a potent anti-VEGF agent. As a consequence, both factors may help to reduce the risk for the development of macular edema theoretically. Nevertheless, results of clinical trials appear inconsistent. Whereas numerous studies reported on limited improvement of function and a short-term effect of macular thickness reduction following surgery,[17,18] others demonstrated a significant benefit for anatomic

0002-9394/$36.00
https://doi.org/10.1016/j.ajo.2018.12.004

and functional measurements in both tractional and nontractional DME even for a long time period.[19–22]

Recent optical coherence tomography (OCT) studies suggested that effectiveness of DME therapy depends on preoperative OCT pattern and thus may be prognostically relevant for the prediction of treatment success.[23–27] Following PPV with ILM peeling, Ichiyama and associates described that postoperative improvement of vision was significantly higher in eyes with subretinal detachment (SRD) than in eyes with cystoid macular edema (CME) or a combination of both patterns with additional sponge-like diffuse retinal thickening (SDRT), whereas eyes with SDRT alone showed no improvement of vision after PPV.[23]

Given that pathologic changes of the vitreous humor and the VMI play a prominent role in diabetic retinopathy, it is of particular interest whether vitreous cortex and VMI characteristics differ according to the type of DME and may potentially help predict the result of a surgical intervention.

The purpose of this study was to characterize cellular structures and extracellular matrix (ECM) components at the VMI in eyes with center-involved tractional and nontractional DME by immunocytochemistry and transmission electron microscopy, and to correlate these findings with spectral-domain OCT (SDOCT) criteria. To further clarify the role of VMI pathology, we analyzed intraretinal biomarkers and clinical data of patients that underwent PPV with ILM removal for DME.

PATIENTS AND METHODS

THIS IS AN INTERVENTIONAL CLINICOPATHOLOGIC INVESTIgation of surgically excised ERM and ILM specimens removed during standard vitrectomy from 27 eyes of 26 patients with DME between January 2008 and December 2014 at the Department of Ophthalmology, Ludwig-Maximilians-University, Munich, Germany. Selection of specimens obtained from patients with DME was consecutive and in retrospect using our register of the Vitreoretinal Pathology Unit of Ludwig-Maximilians-University, Munich, Germany. By flat-mount preparation, all specimens were processed for phase contrast microscopy, interference microscopy, and immunocytochemistry. For transmission electron microscopy, specimens were prepared by ultrathin serial sectioning. Clinical data and SDOCT data were retrospectively analyzed and correlated. This study was approved by the Institutional Review Board and the Ethics Committee of the Ludwig-Maximilians-University and was conducted in accordance with the tenets of the Declaration of Helsinki.

We included specimens obtained from eyes that underwent macular surgery with ILM peeling for center-involved DME when fulfilling the following criteria: (1) postoperative follow-up period of at least 6 months, (2) complete documentation of pre- and postoperative SDOCT examinations, and (3) no other pathology such as macular hole, vitreous hemorrhage, retinal detachment, age-related macular degeneration, inflammatory disease, vascular occlusion, high myopia, or trauma. Recommendation of vitrectomy with membrane peeling was based on (1) the progression of clinical course such as significant decrease in visual acuity during preoperative follow-up period and/or (2) significant impairment of quality of daily life by metamorphopsia and/or (3) nonresponse to pretreatment such as intravitreal pharmacotherapy and/or laser photocoagulation.

Patients' records were reviewed for age, sex, type and duration of diabetes, baseline HbA1c, previous laser coagulation, past medical history including previous intraocular surgery, intravitreal injections, and lens status, as well as preoperative and final best-corrected visual acuity. Status of the vitreous humor was documented as intraoperatively assessed by the surgeon and verified by OCT analysis. In retrospect, none of the eyes had ultrasound examination for differentiation of complete or incomplete posterior vitreous detachment (PVD). Postoperative clinical course was reviewed for functional and anatomic outcomes as well as for further surgical interventions.

Analysis of SDOCT was based on retrospective reevaluation of volume scans with documentation of the type of DME as previously reported[23]: SDRT, CME, SRD, and the combination of all characteristics (FULL). The VMI was analyzed for presence of contractile ERM or thickened vitreous cortex (tVC), and for central macular thickness (CMT).

Statistical analysis was performed using IBM SPSS Statistics Version 25 (IBM Germany, Ehningen) and $P < .05$ was considered statistically significant.

• **SURGICAL PROCEDURE AND SPECIMEN REMOVAL:** All patients underwent a standard 23 gauge PPV with peeling of both epiretinal tissue and the ILM. If not present, induction of PVD was initiated by suctioning with the vitrectomy probe over the optic disc and the posterior pole, and was then continued peripherally. In all eyes membrane removal was performed using Brilliant Blue G (0.2 mL, brilliant peel; Geuder, Heidelberg, Germany). In a subset of patients combined phacovitrectomy was performed depending on cataract formation. In these cases, lens surgery was followed by vitrectomy. Panretinal laser photocoagulation or gas tamponade was performed in eyes with active neovascularization or retinal hole formation. None of the patients received periocular or intraocular injection of long-acting steroids during or at the end of surgery.

• **IMMUNOCYTOCHEMISTRY:** All excised specimens were immediately placed into a mixture of 2% paraformaldehyde and 0.1% glutaraldehyde in 0.1 M phosphate-buffered saline (PBS) (pH 7.4). For immunocytochemistry, specimens were rinsed with 0.1 M PBS and incubated with 0.1 M pepsin for 10 minutes at room temperature. After washing, specimens were processed with normal donkey serum

TABLE 1. Primary Antibodies Used in Incubation of Specimens and Corresponding Target Structure

Primary Antibodies	Target Structure	Trade Name
α-smooth muscle actin (α-SMA)	Myofibroblasts	StCruz sc-130617 (mouse)
MMP-2	Matrix metalloproteinase-2	Millipore AB19167 (rabbit)
MMP-9	Matrix metalloproteinase-9	StCruz sc-21733 (mouse)
CD-45	Hyalocytes	StCruz sc-1123 (goat)
		StCruz sc-20056 (mouse)
		StCruz sc-25590 (rabbit)
CD-64	Hyalocytes	StCruz sc-31216 (goat)
		StCruz sc-1184 (mouse)
		StCruz sc-15364 (rabbit)
CD-68	Macrophages	StCruz sc-7082 (goat)
		DAKO M 0814 (mouse)
Glial fibrillary acidic protein (GFAP)	Glial cells	StCruz sc-6870 (goat)
		StCruz sc-9973 (mouse)
		DAKO Z 0334 (rabbit)
Vimentin	Glial cells	SIGMA V 4630 (goat)
		DAKO M 0725 (mouse)
Cytokeratin-8	Retinal pigment epithelial cells	Sigma C5301 (mouse)
Collagen type I	Extracellular matrix	StCruz sc-25374 (goat)
Collagen type II	Extracellular matrix	Biotrend BT 2150-0060 (rabbit)
Collagen type III	Extracellular matrix	Biotrend BT 2150-0100 (rabbit)

(dilution, 1:20) in PBS, 0.5% bovine serum albumin (BSA), 0.1% Triton X-100, and 0.1% sodium azide for 2 hours at room temperature. Thereafter, they were washed with PBS and incubated with primary antibodies (Table 1).

Antifading mounting medium 4′,6-diamidino-2-phenylindol (DAPI; AKS-38448; Dianova, Hamburg, Germany) was used for cell nuclei staining. All specimens were prepared as whole flat mounts after fixation. Under a stereomicroscope (MS 5; Leica, Wetzlar, Germany), the specimens were placed onto glass slides. To show the maximum area of their surface, specimens were unfolded using glass pipettes. If possible, specimens were segmented to use all antibody combinations per specimen. Primary antibodies were diluted according to manufacturer's instructions. We used labeling combinations of 3 antibodies. The second antibodies (donkey anti-mouse CY3, donkey anti-rabbit CY2, donkey anti-goat CY5; Dianova, Hamburg, Germany) were added together, each in 1:100 PBTA (phosphate buffered saline 0.1M Sörenses, 0.5% Bovine Serum Albumin Sigma A-9647, 0.1% Triton-X-100 Sigma X-100, 0.1% sodium azide Sigma S-8032). For negative control, primary antibodies were substituted with an isotope control antibody (IgG; GeneTex, Eching, Germany; IgG1; DAKO, Hamburg, Germany; IgG2a; DAKO, Hamburg, Germany; Sigma-Aldrich, Taufkirchen, Germany). All specimens were processed following the identical procedure.

The manual cell counting was performed using ImageJ (National Institutes of Health, Bethesda, Maryland, USA). Specimens were analyzed by phase contrast microscopy, interference microscopy, and fluorescence microscopy using a modified fluorescence microscope (Leica DM 2500, Leica Microsystems, Wetzlar, Germany). For photographic documentation, a digital camera was used to image the specimens at magnifications between ×50 and ×400 (ProgRes CF; Jenoptik, Jena, Germany).

• **TRANSMISSION ELECTRON MICROSCOPY:** After fixation and flat-mount preparation with immunocytochemical staining procedures, specimens were processed for postfixation with osmium tetroxide 2% (Dalton's fixative). Dehydration in graded series of ethanol and embedding in epoxy resin Epon 812 followed. Ultrathin sections of 60 nm were contrasted with uranyl acetate and lead citrate. Analysis and imaging were independently performed by 2 masked observers (F.H., R.S.) using a Zeiss light microscope and a Zeiss EM 9 S-2 electron microscope with wide-angle dual-speed CCD camera and documentation (Zeiss, Jena, Germany). Measurement of collagen fibrils and analysis was performed using Adobe Photoshop CS6 (Adobe Systems Software Ireland Limited, Dublin, Ireland) and SPSS 25.0 (IBM Germany, Ehningen), respectively.

RESULTS

• **CLINICAL DATA ANALYSIS:** Patients' age ranged between 21 and 81 years with a mean of 62.2 ± 14.2 years (median 65 years). Sixteen patients were male, 10 patients were female, and operations were done on 11 right and 16 left eyes. Mean follow-up period was 17 ± 10 months (median 13; range: 6-40 months). Table 2 demonstrates the main clinical data of all patients at baseline and follow-up.

TABLE 2. Main Clinical Data of All Patients at Baseline and Follow-up

ID	Age/Sex/Eye	DME Pattern (OCT)	Diabetic Retinopathy	DM Type	Laser Treatment		Intravitreal Therapy		Lens Status		BCVA (logMAR)		VA Gain in Lines	FU in Months
					Preop	Postop	Preop	Postop	Preop	Postop	Preop	Last-FU		
1	72/M/OS	SDRT	PDR	II	Panretinal	-	-	-	IOL	IOL	1.7	0.7	10	18
2	72/F/OS	SDRT	NPDR	II	-	-	BVZ	DEX	Phakic	IOL	0.8	0.8	0	24
3	67/M/OD	SDRT	PDR	II	Focal	-	-	-	Phakic	IOL	1.5	1.0	5	23
4	60/F/OS	SDRT	PDR	II	Panretinal	-	-	-	Phakic	IOL	0.7	0.5	2	40
5	77/F/OS	SDRT	PDR	II	Panretinal	-	-	-	Phakic	IOL	1.7	1.0	7	12
6	67/M/OS	SDRT	PDR	II	Panretinal	-	BVZ	-	IOL	IOL	1.3	2.0	-7	6
7	74/M/OS	SDRT	PDR	II	-	-	-	RNB	IOL	IOL	0.4	0.2	2	24
8	59/M/OD	SDRT	NPDR	II	-	-	-	BVZ	Phakic	IOL	0.6	1.0	-4	7
9	75/M/OS	SDRT	PDR	II	Panretinal	-	RNB	-	Phakic	IOL	0.7	0.1	6	32
10	56/F/OS	SDRT	PDR	II	Panretinal	-	RNB	-	Phakic	IOL	1.0	0.3	7	8
11	65/M/OS	SDRT	PDR	II	-	-	BVZ	-	IOL	IOL	1.0	1.0	0	14
12	63/M/OD	SDRT	NPDR	II	-	-	-	-	Phakic	IOL	1.0	0.4	6	14
13	78/F/OS	CME	NPDR	II	-	-	-	-	Phakic	IOL	0.5	0.3	2	10
14	67/M/OD	CME	NPDR	II	-	-	-	-	Phakic	IOL	0.3	0.2	1	24
15	71/F/OD	CME	PDR	II	Panretinal	Focal	-	-	Phakic	IOL	0.6	0.2	4	12
16	29/M/OS	CME	PDR	I	Panretinal	-	BVZ	-	Phakic	Phakic	0.7	0.2	5	24
17	81/F/OS	CME	NPDR	II	-	-	BVZ	-	IOL	IOL	1.3	0.8	5	6
18	69/M/OS	CME	PDR	I	-	-	-	-	Phakic	IOL	0.3	0.1	2	11
19	65/M/OD	CME	PDR	I	Panretinal	-	RNB	-	IOL	IOL	1.0	0.8	2	6
20	64/M/OD	CME	PDR	II	Panretinal	-	-	-	Phakic	IOL	1.4	1.0	4	10
21	41/F/OS	CME	PDR	I	Panretinal	Panretinal	-	-	Phakic	Phakic	0.2	0.5	-3	10
22	48/M/OD	FULL	PDR	II	Panretinal	-	-	-	Phakic	IOL	1.5	0.0	15	24
23	66/F/OS	FULL	PDR	II	Panretinal	-	-	RNB	IOL	IOL	1.0	0.6	4	11
24	63/M/OS	FULL	NPDR	II	Focal	-	-	-	IOL	IOL	0.4	0.2	2	24
25	59/M/OD	FULL	PDR	II	-	-	BVZ	-	Phakic	IOL	1.3	1.0	3	38
26	50/M/OD	FULL	PDR	II	-	-	RNB	-	Phakic	IOL	1.7	1.7	0	9
27	21/F/OD	FULL	PDR	I	Panretinal	-	-	-	Phakic	Phakic	0.7	0.1	6	13

BCVA = best-corrected visual acuity; BVZ = bevacizumab; CME = cystoid macular edema; DEX = dexamethasone implant 0.7 mg; DM = diabetes mellitus; DME = diabetic macular edema; FULL = combination of SDRT, CME, and serous retinal detachment; FU = follow-up; IOL = intraocular lens; NPDR = nonproliferative diabetic retinopathy; OCT = optical coherence tomography; PDR = proliferative diabetic retinopathy; Postop = postoperative; Preop = preoperative; RNB = ranibizumab; SDRT = sponge-like diffuse retinal thickening; VA = visual acuity.

Five of 26 patients (19%) presented with diabetes mellitus type I and 21 patients (81%) with type II. Mean duration of disease beginning from first diagnosis was documented with 18.7 ± 13.4 years (median 12; range 1-45 years). Mean HbA1c levels were 7.5% ± 0.8% (median 7.8%; range 5.7%-8.4%). Both subgroups of diabetic retinopathy were represented: 7 eyes (26%) with nonproliferative diabetic retinopathy (NPDR) and 20 eyes (74%) with proliferative diabetic retinopathy (PDR).

Fifteen eyes (56%) had history of previous laser treatment with panretinal photocoagulation. History of focal laser treatment was documented in 2 eyes (7%). Ten eyes (37%) had not undergone laser treatment. In total, 10 eyes (37%) received intravitreal anti-VEGF injection (bevacizumab or ranibizumab), and none of the patients received a prior surgery. Postoperatively, 3 eyes received anti-VEGF injections and 1 eye dexamethasone implant owing to persistent DME. Postoperative complications included vitreous hemorrhage in 2 eyes.

Preoperatively, 19 eyes (70%) were phakic and 8 eyes (30%) were pseudophakic. At last follow-up, 3 eyes (11%) remained phakic. In 16 cases (59%), phakic eyes underwent PPV combined with cataract surgery using phacoemulsification and implantation of an intraocular lens. Eyes operated by a combination of PPV with cataract surgery showed no significant difference in visual acuity change compared to eyes that underwent PPV alone (Mann-Whitney test: $P = .53$).

Preoperatively, the mean best-corrected visual acuity (BCVA) was logMAR 0.93 ± 0.5 (median 1.0; range 1.7-0.2 logMAR; Snellen 20/200). Following PPV with ILM peeling at last follow-up, mean BCVA increased to logMAR 0.62 ± 0.5 (median 0.5; range 0-2.0; Snellen 20/80), resulting in a significant VA improvement of 3.2 ± 4.3 lines (median 3 lines; range -7 to 15) postoperatively (Wilcoxon test: $P = .002$). Postoperative visual acuity was significantly better in eyes with a follow-up of ≤10 months compared to eyes with a follow-up of

TABLE 3. Optical Coherence Tomography and Ultrastructural Analysis

	SDRT (N = 12)	CME (N = 9)	FULL (N = 6)
State of the vitreous			
Posterior vitreous			
Attached	7 (58%)	6 (67%)	3 (50%)
Partial detachment	3 (25%)	1 (11%)	1 (17%)
Complete detachment	2 (17%)	2 (22%)	2 (33%)
Spectral-domain optical coherence tomography			
Vitreomacular interface			
ERM	12 (100%)	6 (67%)	5 (83%)
tVC	3 (25%)	2 (22%)	3 (50%)
Intraretinal biomarker			
HRD	8 (67%)	5 (56%)	3 (50%)
DRIL	12 (100%)	8 (89%)	6 (100%)
EZ defect	7 (58%)	3 (33%)	3 (50%)
Central macular thickness			
Preoperative, mean ± SD (range) μm	424.1 ± 150.5 (201-614)	432.8 ± 92.3 (326-588)	551.6 ± 161.7 (409-829)
Postoperative, mean ± SD (range) μm	332.8 ± 96.8 (182-570)	323.8 ± 39.1 (248-369)	393.8 ± 143.9 (271-611)
Whole flat mounts			
Cell nuclei staining			
Cell density,[a] median (range)	92 (12-381)	71 (5-396)	199 (6-350)
Homogenous cell distribution	5 (42%)	3 (33%)	4 (67%)
Cell cluster	7 (58%)	6 (67%)	2 (33%)
Ultrastructural features on transmission electron microscopy			
Retinal side of the ILM			
Small cell debris	3 (25%)	0	0
Whole retinal cells	0	0	0
Vitreal side of the ILM			
Hyalocytes	10 (83%)	8 (89%)	5 (83%)
Myofibroblasts	10 (83%)	4 (44%)	6 (100%)
Glial cells	8 (67%)	6 (67%)	2 (33%)
Collagen types			
NVC	10 (83%)	6 (67%)	3 (50%)
NFC	6 (50%)	6 (67%)	3 (50%)
FLSC	4 (33%)	0	0

CME = cystoid macular edema; DRIL = disorganization of retinal inner layers; EZ = ellipsoid zone; FLSC = fibrous long-spacing collagen; FULL = combination of SDRT, CME, and serous retinal detachment; ERM = epiretinal membrane; HRD = hyperreflective dots; ILM = internal limiting membrane; NFC = newly formed collagen; NVC = native vitreous collagen; SDRT = sponge-like diffuse retinal thickening; tVC = thickened vitreous cortex.

[a]Cell number/mm^2.

>10 months (Mann-Whitney test: $P = .027$). Concerning the change of BCVA, there were no significant correlations found with age, type of diabetes, grade of retinopathy, or state of the lens or vitreous, nor with presence and cell pattern of ERM, type of edema, or preoperative therapy (Mann-Whitney test: $P > .05$).

• **OPTICAL COHERENCE TOMOGRAPHY ANALYSIS:** By OCT analysis as presented in Table 3, we found 3 of 4 reported subtypes of DME: SDRT (Figure 1, Top), CME (Figure 2, Top), and the combination of SDRT, CME, and SRD (FULL) (Figure 3, Top). Twelve eyes (44%) were seen with an SDRT, 9 eyes (33%) had a CME, and 6 eyes (22%) were found with a combination of SDRT, CME, and SRD. None of our patients presented with SRD alone.

Concerning intraretinal biomarker, we found hyperreflective dots (HRD) in 16 eyes (59%), a disorganization of retinal inner layers (DRIL) in all eyes except for 1 eye with CME (96%), and ellipsoid zone (EZ) defects in 13 eyes (48%). There was no correlation between HRD and the type of DME, nor between EZ defects and DRIL with the type of DME. However, integrity of EZ significantly correlated with better visual acuity gain compared to EZ defects (Mann-Whitney test: $P = .014$).

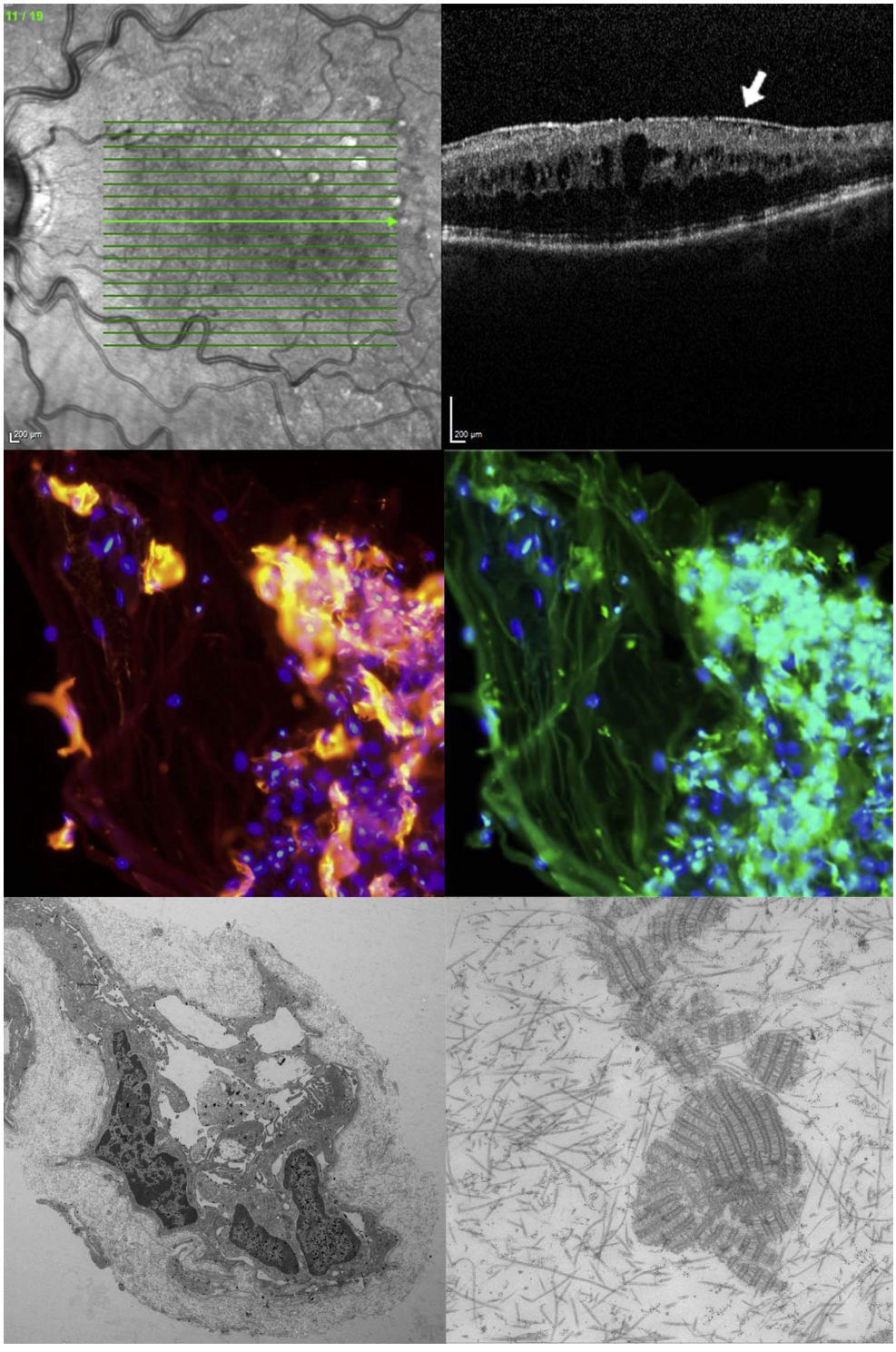

FIGURE 1. (Top) Infrared fundus image and corresponding macular spectral-domain optical coherence tomography B-scan showing sponge-like diffuse retinal thickening and presence of epiretinal membrane (arrow). (Middle left) Immunocytochemical staining after flat-mount preparation with anti-α-smooth muscle actin (anti-α-SMA)-positive (yellow) staining in co-localization with anti-collagen I (red) merged with cell nuclei staining (blue) (magnification ×200) revealed presence of active myofibroblasts. (Middle right) Immunocytochemical staining showing presence of CD45-positive hyalocytes (green) with cell nuclei staining (blue), corresponding to area at middle left (magnification ×200). (Bottom left) Transmission electron micrograph showing epiretinal cells, predominantly myofibroblasts interposed in thick native vitreous collagen strand (magnification ×4400). (Bottom right) Transmission electron microscopy revealed presence of fibrous long-spacing collagen embedded in native vitreous collagen demonstrating a remodeling process of vitreous collagen (magnification ×30 000).

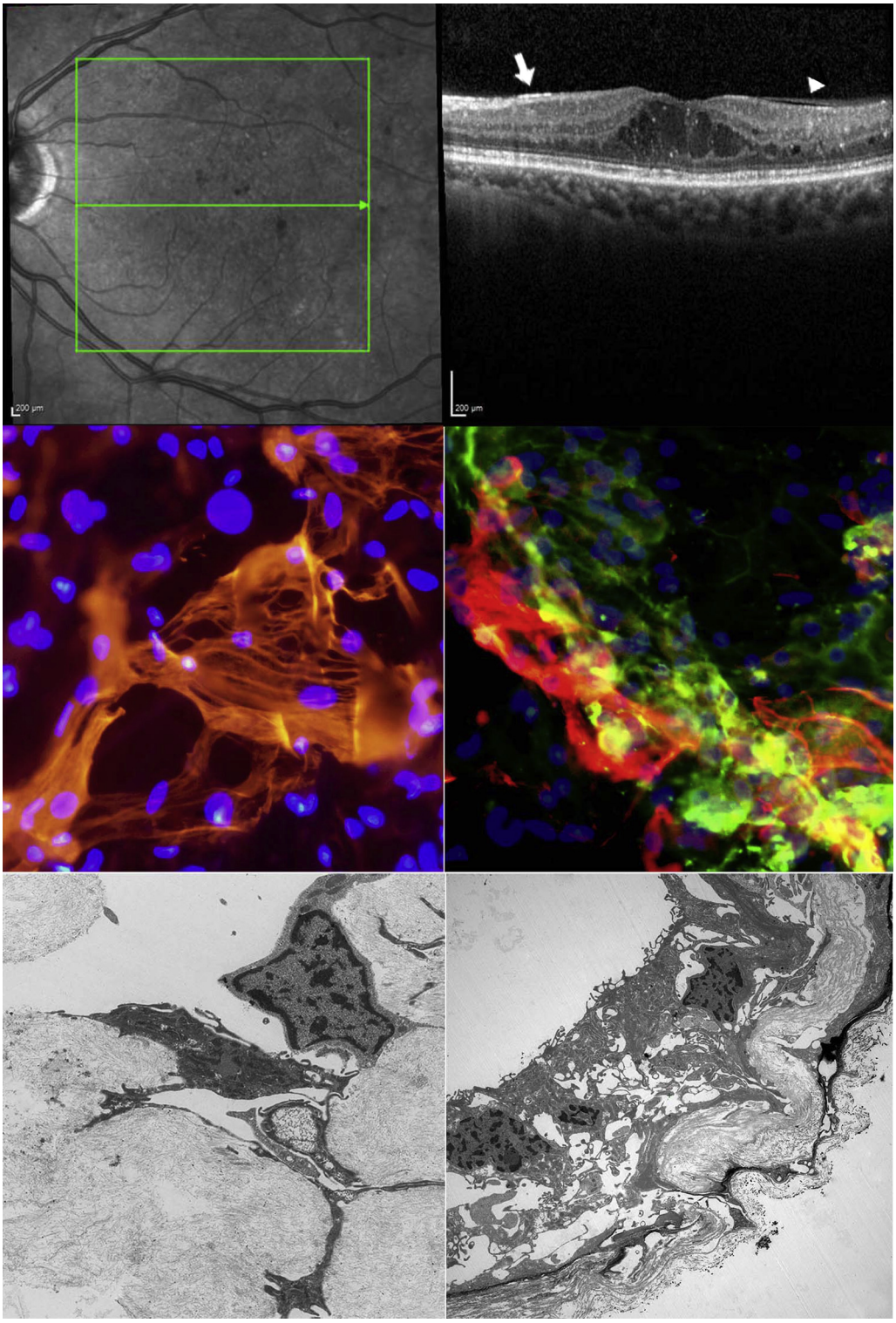

FIGURE 2. (Top) Infrared fundus image and corresponding macular spectral-domain optical coherence tomography B-scan showing cystoid macular edema with epiretinal membrane (arrow) and thickened vitreous cortex (arrowhead). (Middle left) Immunocytochemical staining after flat-mount preparation with anti-α-smooth muscle actin (anti-α-SMA)-positive (red) staining showing intracytoplasmic actin filaments in higher magnification merged with cell nuclei staining (blue) (magnification ×400). (Middle right) Immunocytochemical staining demonstrates anti-α-SMA, anti-collagen I, and collagen III in combination with cell nuclei staining (blue) (magnification ×400). (Bottom left) Transmission electron micrograph presents epiretinal myofibroblasts and hyalocytes with abundance of vitreous collagen (magnification ×7000). (Bottom right) Transmission electron microscopy revealed multilayered cell proliferations with newly formed collagen and folding of collagen strands (magnification ×3000).

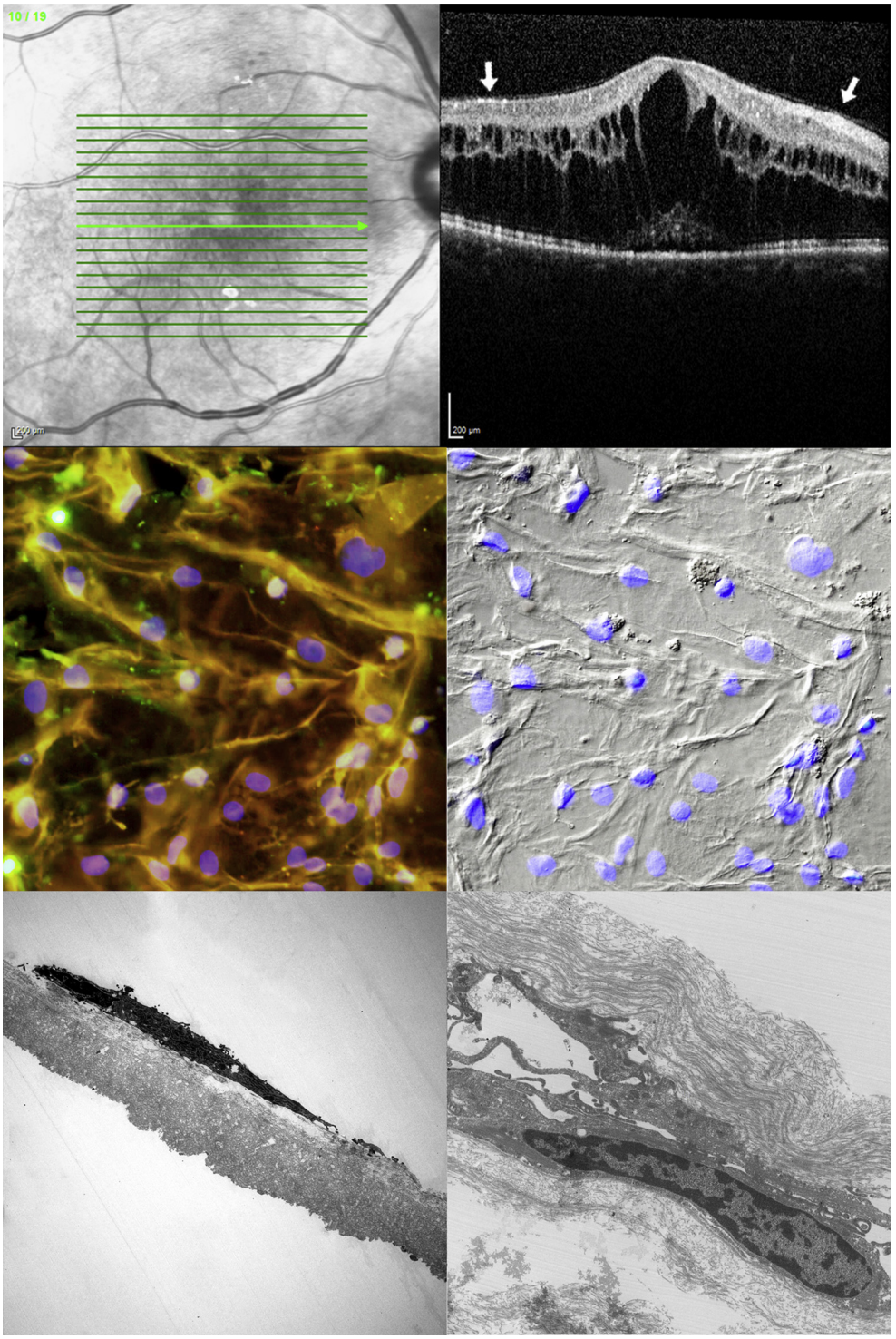

FIGURE 3. (Top) Infrared fundus image and corresponding macular spectral-domain optical coherence tomography B-scan showing combination of cystoid and diffuse macular edema and subretinal detachment with an attached posterior vitreous (arrow). (Middle left) Immunocytochemical staining after flat-mount preparation with anti–matrix metalloproteinase-2 (green) and anti–matrix metalloproteinase-9 (yellow) in co-localization merged with cell nuclei staining (blue) (magnification ×400). (Middle right) Interference microscopy of flat-mounted tissue illustrating same area as middle left with cell nuclei staining (blue). (Bottom left) Transmission electron microscopy showing single hyalocyte on the vitreal side of the internal limiting membrane situated on collagen fibrils (magnification ×7000). (Bottom right) Transmission electron micrograph showing hyalocytes embedded in vitreous cortex collagen strands (magnification ×12 000).

TABLE 4. Analysis of Optical Coherence Tomography Patterns and Immunocytochemical Staining Characteristics in Eyes With Diabetic Macular Edema

	Immunocytochemical Staining Characteristics of Flat Mounts											
										Collagen Type		
SDOCT Findings	SMA	Vim	GFAP	CD45	CD64	CD68	CK8	MMP-2	MMP-9	I	II	III
DME patterns												
Sponge-like diffuse retinal thickening (SDRT)	+	+	+	+	+	-	+	+	+++	+	+	+
Cystoid macular edema (CME)	+++	+	+	+	+	-	+	+	+++	+	+	+
Combination of SDRT, CME, and serous retinal detachment (FULL)	+	+	+	+	-	-	+	+	+	+	+	+
VMI features												
Epiretinal membrane (ERM)	+++	++	+	+	+	-	+	+	+++	+	+	+
Thickened vitreous cortex (tVC)	+	+	+	+	-	-	-	+	+	+	+	+

CD = cluster of differentiation; CK = cytokeratin; DME = diabetic macular edema; GFAP = glial fibrillary acidic protein; MMP = matrix metalloproteinase; SMA = α-smooth muscle actin; Vim = vimentin; VMI = vitreomacular interface.

Regarding the state of the vitreous humor, PVD was determined as complete PVD in 5 eyes (19%) and partial PVD in 6 eyes (22%). In 16 eyes (59%) the posterior vitreous was still attached. Epiretinal membranes were found in 23 eyes (85%) and were described as hyperreflective line situated on the retinal surface. Thickened vitreous cortex was documented in 8 eyes (30%). The majority of eyes with tVC showed coexistence of ERM.

Postoperatively, mean CMT showed a significant reduction from preoperative 451.6 ± 139.2 μm (median 476.5 μm; range 201-829 μm) to postoperative 341.4 ± 92.9 μm (median 331.0 μm; range 182-611 μm), with a mean decrease of 110.2 ± 107.6 μm (median 95.0 μm, range: -24 to 337 μm) (Wilcoxon test: $P = .001$). There was no correlation of the change of CMT with change of visual function. Statistical analysis of the amount of CMT reduction revealed no significant correlation but a tendency with the type of DME (FULL > CME > SDRT) (Kruskal-Wallis test: $P = .169$).

We found no statistical difference regarding the reduction of CMT between eyes that underwent phacovitrectomy and vitrectomy-only eyes (Kruskal-Wallis Test: $P = .3$).

• **CELL DISTRIBUTION ANALYSIS:** Mean area of removed specimens per eye was 8.3 ± 7.3 mm^2 (median 5.7 mm^2). Cell distribution analysis revealed cell cluster formation in 15 (56%) eyes and homogenous cell multilayer in 12 (44%) eyes. Cell density ranged from 5 cells/mm^2 to 1741 cells/mm^2 with a mean of 194.9 ± 333.7 cells/mm^2 (median 103 cells/mm^2) (Table 3).

• **IMMUNOCYTOCHEMICAL ANALYSIS:** As demonstrated in Table 4, the majority of specimens showed a positive staining for hyalocyte markers CD45 and CD64. Hyalocytes were often seen in co-localization with α-smooth muscle actin (α-SMA) (Figure 1, Middle). The ECM was tested using different types of collagen (type I, II, and III) all showing positive staining. Myofibroblasts were co-localized with positive staining for α-SMA, collagen I, and collagen III (Figure 2, Middle). We found positive immunostaining for matrix metalloproteinase-9 being superior to immunostaining for matrix metalloproteinase-2 (Figure 3, Middle), especially in eyes with SDRT and CME. Immunolabeling with anti–glial fibrillary acidic protein and anti-vimentin showed a positive reaction as well, whereas retinal pigment epithelium cells were less often demonstrated.

• **ULTRASTRUCTURAL ANALYSIS:** Presence of epiretinal cells was identified in all eyes irrespective of the type of DME, as illustrated in transmission electron micrographs of Figures 1-3. The ILM was characterized by the smooth vitreal and the undulated retinal side. Small retinal cell debris at the retinal side of the ILM has been found in specimens of 3 eyes with SDRT exclusively. Ultrastructural analysis revealed predominance of hyalocytes and myofibroblasts, with frequent presence of fibrous astrocytes. Hyalocytes and myofibroblasts were often embedded in thick collagen strands (Figures 1 and 2). Besides of native vitreous collagen (Figures 1 and 2) there was newly formed collagen (Figure 1, Bottom left) in the majority of specimens. Fibrous long-spacing collagen was seen in SDRT (Figure 1, Bottom right). Topographically, epiretinal cells were described as directly attached to the vitreal side of the ILM or embedded in a strand of vitreous collagen (Figure 2, Bottom).

• **CORRELATION OF ULTRASTRUCTURE AND IMMUNOSTAINING WITH OPTICAL COHERENCE TOMOGRAPHY FINDINGS:** Ultrastructural and immunocytochemical

findings significantly correlated neither with OCT classification of DME type nor with intraretinal HRD, DRIL, or EZ defects. We found multilayered membranes mainly composed of hyalocytes and myofibroblasts that were embedded in masses of collagen. Whereas the amount of cell and collagen deposits on the ILM was variable between cases, the type of cells and the type of collagen did not differ. Eyes with FULL pattern showed the highest density of cellular proliferation compared to SDRT und CME. We demonstrated thick strands of vitreous cortex collagen at the VMI in the majority of eyes combined with a proportion of newly formed collagen in multilayered membranes. Fibrous long-spacing collagen within vitreous collagen fibrils was seen in 4 eyes with SDRT only.

We found no difference regarding the cell distribution pattern in eyes with attached or detached posterior vitreous.

DISCUSSION

IN THE DIABETIC EYE, THE VITREOUS HUMOR UNDERGOES significant changes, including abnormal posterior detachment, abnormal collagen crosslinking, and nonenzymatic glycation at the VMI.[28,29] By immunocytochemical and electron microscopic analysis, this clinicopathologic study compared VMI characteristics of eyes with tractional and nontractional DME and correlated these results with SDOCT findings and clinical data. Patient selection was consecutive and in retrospect using the Register of the Vitreomacular Pathology Unit, Ludwig-Maximilians-University, Munich.

Our results indicate that pathologic fibrocellular changes at the VMI are present in all eyes with DME irrespective of the type of macular edema as classified by SDOCT. Moreover, ultrastructural and immunocytochemical findings correlated neither with HRD nor with DRIL or EZ defects. In accordance with previous studies on epiretinal pathology in diffuse DME,[11,13] we found multilayered membranes mainly composed of hyalocytes and myofibroblasts that were embedded in masses of collagen. Fibrous long-spacing collagen within vitreous collagen fibrils was seen in 4 eyes only, representing a remodeling process of vitreous cortex that was previously suggested to be age-related.[30] It is noteworthy that the amount of cells and the complexity of cellular membranes varied between eyes with and without ERMs, but there was no difference in the kind of cells and ECM components that were found at the VMI in tractional and nontractional DME.

In terms of immunostaining, eyes with SDRT and CME were most intensely positive for active myofibroblasts and the enzyme matrix metalloproteinase-9 (MMP-9). Matrix metalloproteinases are a family of zinc ion–binding calcium-dependent endopeptidases that are involved in degrading ECM components, which is a key point in the angiogenic switch of diabetic retinopathy.[31–33] MMPs are able to regulate VEGF bioavailability and thereby promote a progression to proliferative disease. An upregulation of MMPs is known to be associated with angiogenesis and progression to proliferative disease.[34]

In healthy eyes, hyalocytes are distributed as single cells within the vitreous cortex at an average distance of 20-50 μm from the inner surface of the retina.[35,36] These cells are known to be resident vitreous cells that derive from the hematopoietic monocyte/macrophage lineage. In a quiescent state, they possess thin and elongated cell bodies and their cell membranes contain CD45, as previously demonstrated in epiretinal membranes of eyes with macular holes and macular pucker.[37,38] Owing to their role in ECM synthesis and regulation of intraocular immunoreactions, hyalocytes modulate inflammation in vitreoretinal diseases.[35] In pathologic eyes, hyalocytes were shown to produce VEGF and can transdifferentiate into myofibroblasts.[30,39] Myofibroblasts are known for their contractive properties and their ability to produce newly formed collagen, both demonstrated in this study by the co-localization of α-SMA and collagen type I. Myofibroblasts can transdifferentiate from numerous cell types. Our finding of co-localization of CD45 and α-SMA suggests an epithelial/mesenchymal transdifferentiation of hyalocytes into myofibroblasts. Furthermore, hyalocytes were found directly neighboring myofibroblasts embedded in a thick layer of native vitreous collagen or in a minor proportion directly situated to the vitreous side of the ILM. Multilayered ERMs composed of hyalocytes, myofibroblasts, and native vitreous collagen point to the presence of vitreoschisis, consistent with other publications in the past.[11,13]

Vitreoschisis represents a split of the posterior vitreous cortex in anomalous PVD, leaving a layer of vitreous collagen fibrils on the retinal surface. Moreover, surgical intervention during PPV can also lead to vitreoschisis induced by suctioning with the vitrectomy probe over the optic disc. In accordance with previous studies, the majority of eyes of this series were found with attached vitreous. In eyes with detached or partially detached posterior vitreous, the finding of multilayered fibrocellular membranes indicated the presence of vitreoschisis. In eyes with attached posterior vitreous, fibrocellular membranes at the ILM demonstrated advanced pathologic changes at the VMI in diabetic eyes despite persistent attachment of posterior vitreous.

The rationale of removing vitreous by PPV appears not only closely related to removal of vitreous collagen network but also to the various functions of hyalocytes in the cascade of pathologic changes in diabetic eyes. It is well known that PPV improves oxygenation of inner retinal layers with an increase of the vitreal diffusion coefficient and a consecutive

decrease of VEGF concentration and other DME-promoting cytokines, especially in the premacular area, but with a stable effectiveness of intravitreal therapy after vitrectomy.[40,41] It is also well accepted that PPV with vitreous cortex removal and ILM peeling is beneficial in terms of traction release. However, there is little understanding on the function of intra- and extraretinal cell components in the course of disease. Potentially, cellular structures such as hyalocytes play a more prominent role in DME development and progression than previously expected.

According to immunocytochemical and ultrastructural findings of this study, one might argue for an early surgical intervention in order to remove cellular structures such as hyalocytes that were shown to be involved in pathogenesis of diabetic retinopathy and DME progression. Currently, indication of PPV in eyes with DME depends on traction formation at the VMI or on persistence of macular edema following intensive pharmacotherapy with anti-VEGF or steroids. Owing to inconsistent anatomic and functional postoperative results after PPV, there still is a debate on the role of PPV in the algorithm of treatment, especially in eyes with nontractional DME.[17,21,23] Functional results of this study after PPV with ILM peeling emphasize the postulated benefit of removing vitreous and especially the vitreomacular interface in eyes with DME. Those results, however, should be considered with caution owing to the retrospective design of this study. Most eyes showed a significant improvement of visual acuity over a mean follow-up period of 17 months. Looking further into the data, there was a difference in postoperative visual acuity comparing eyes with shorter and longer follow-up. Eyes that were followed for less than 11 months showed better vision than eyes with more than 11 months of follow-up. Consequently, our study results cannot prove that the effect of functional improvements after PPV remain stable over a long-term period in all eyes. We hypothesize that once DME is initiated, other factors than vitreous changes may also influence the course of disease, such as the HbA1c level, which was shown to affect the resolution of macular edema after PPV.[42,43]

In addition, risk assessment of the surgical intervention, including the necessity of ILM peeling, is a matter of controversy. When retinal architecture is disorganized and weakened by a longstanding and chronic DME, removal of the ILM during PPV without injuring retinal layers can be a challenging procedure. Retinal damage such as rupturing intraretinal cystoid spaces might be suspected when pulling off the basal lamina of Müller cells during macular surgery. Although Kumagai and associates reported that PPV significantly improves vision in eyes with DME, they found no improvement of functional results comparing PPV with ILM peeling and PPV alone in corresponding eyes of the same patients.[21] With regard to the ILM peeling procedure, our ultrastructural analysis revealed no significant cell debris at the retinal side of ILM. Thus, ILM peeling in eyes with DME appears a safe procedure, since there was no evidence of de-roofing intraretinal cystoid spaces in this study.

Limitations of the study include its retrospective analysis of clinical data, minor information on systemic factors during the period of follow-up, and the lack of angiographic examination results for proper evaluation of ischemia in eyes with DME. In terms of changes in visual acuity, the retrospective study design restricts the interpretation of the functional results with regard to the accuracy of obtaining BCVA. Furthermore, collection of tissue during PPV might have been incomplete and could have led to incorrect numbers of cell density measurements. The event of combined PPV with cataract extraction in many cases of this series may have influenced the functional results, although we have found no difference in visual gain between eyes with and without combination surgery by statistical analysis.

In conclusion, pathologic VMI changes were presented in all eyes irrespective of the OCT classification of DME type or the presence of tractional ERM. Composition of fibrocellular membranes at the VMI indicated remodeling of vitreous cortex and transdifferentiation of hyalocytes into myofibroblasts. Cellular changes at the VMI in diabetic eyes may explain the firm adherences between vitreous and retinal ILM surface. According to our results, PPV with ILM peeling improves visual acuity and macular thickness without safety concerns over a moderate follow-up period, mainly correlating to the presence of outer photoreceptor defects. There were no significant differences in anatomic and functional improvement comparing tractional and nontractional DME. Ultrastructural and immunocytochemical findings of this study might argue for an early surgical intervention in eyes with DME irrespective of the presence of traction formation imaged by SDOCT. The influence of systemic factors on visual outcome remains to be evaluated, and comparative studies will be needed to elucidate prognostic factors for surgical intervention in eyes with DME.

FUNDING/SUPPORT: NO FUNDING OR GRANT SUPPORT. FINANCIAL DISCLOSURES: FELIX HAGENAU: TRAVEL REIMBURSEMENTS by Allergan plc. Christos Haritoglou: honoraria and consulting fees by Allergan plc, Bayer Pharma AG, Novartis AG. Siegfried G. Priglinger: travel reimbursements and speaker fees by Allergan plc, Bayer Pharma AG, Novartis AG, Heidelberg Engineering, Oertli Instrumente AG, DORC. Armin Wolf: travel reimbursements by Novartis AG, Oertli Instrumente AG. Ricarda G. Schumann: travel reimbursements and speaker fees by Allergan plc, Bayer Pharma AG, Novartis AG, Heidelberg Engineering. The following authors have no financial disclosures: Denise Vogt, Jean Ziada, and Stefanie R. Guenther. All authors attest that they meet the current ICMJE criteria for authorship.

REFERENCES

1. Yau JWY, Rogers SL, Kawasaki R, et al. Global prevalence and major risk factors of diabetic retinopathy. *Diabetes Care* 2012;35:556–564.
2. Schmidt-Erfurth U, Garcia-Arumi J, Bandello F, et al. Guidelines for the management of diabetic macular edema by the European Society of Retina Specialists (EURETINA). *Ophthalmologica* 2017;237(4):185–222.
3. Bressler SB, Melia M, Glassmann AR, et al. Ranibizumab plus prompt or deferred laser for diabetic macular edema in eyes with vitrectomy before anti-vascular endothelial growth factor therapy. *Retina* 2015;35(12):2516–2528.
4. Browning DJ, Lee C, Stewart MW, et al. Vitrectomy for center-involved diabetic macular edema. *Clin Ophthalmol* 2016;10:735–742.
5. Jackson TL, Nicod E, Angelis A, et al. Pars plana vitrectomy for diabetic macular edema. A systematic review, meta-analysis, and synthesis of safety literature. *Retina* 2017; 37(5):886–895.
6. Jackson TL, Johnston RL, Donachie PH, et al. The Royal College of Ophthalmologists' National Ophthalmology Database Study of vitreoretinal surgery: Report 6, Diabetic vitrectomy. *JAMA Ophthalmol* 2016;134(1):79–85.
7. Patelli F, Radice P, Giacomotti E. Diabetic macular edema. *Dev Ophthalmol* 2014;54:164–173.
8. Capitao M, Soares R. Angiogenesis and inflammation crosstalk in diabetic retinopathy. *J Cell Biochem Res* 2016;17(11): 2443–2453.
9. Kovacs K, Marra KV, Yu G. Angiogenic and inflammatory vitreous biomarkers associated with increasing levels of retinal ischemia. *Invest Ophthalmol Vis Sci* 2015;56:6523–6530.
10. Loukovaara S, Nurkkala H, Tamene F, et al. Quantitative proteomics analysis of vitreous humor from diabetic retinopathy patients. *J Proteome Res* 2015;14:5131–5143.
11. Gandorfer A, Rohleder M, Grosselfinger S, et al. Epiretinal pathology of diffuse diabetic macular edema associated with vitreomacular traction. *Am J Ophthalmol* 2005;139(4):638–652.
12. Ophir A, Martinez MR. Epiretinal membranes and incomplete posterior vitreous detachment in diabetic macular edema, detected by spectral-domain optical coherence tomography. *Invest Ophthalmol Vis Sci* 2011;52(9):6414–6420.
13. Matsunaga N, Ozeki H, Hirabayashi Y, et al. Histopathologic evaluation of the internal limiting membrane surgically excised from eyes with diabetic maculopathy. *Retina* 2005; 25(3):311–316.
14. Gandorfer A. Diffuse diabetic macular edema: pathology and implications for surgery. *Dev Ophthalmol* 2007;38:88–95.
15. Sebag J. Age related changes in human vitreous structure. *Graefes Arch Clin Exp Ophthalmol* 1987;225:89–93.
16. Stefansson E. Physiology of the vitreous. *Graefes Arch Clin Exp Ophthalmol* 2009;247:147–163.
17. Hoerauf H, Brüggemann A, Muecke M, et al. Pars plana virectomy for diabetic macular edema. Internal limiting membrane delamination vs posterior hyaloid removal. A prospective randomized trial. *Graefes Arch Clin Exp Ophthalmol* 2011;249(7):997–1008.
18. Figueroa MS, Contreras I, Noval S. Surgical and anatomical outcomes of pars plana vitrectomy for diffuse non-tractional diabetic macular edema. *Retina* 2008;28:420–426.
19. Yamamoto T, Naoko A, Takeuchi S. Vitrectomy for diabetic macular edema: the role of posterior vitreous detachment and epimacular membrane. *Am J Ophthalmol* 2001;132(3):369–377.
20. Iglicki M, Lavaque A, Ozimek M, et al. Biomarkers and predictors for functional and anatomic outcomes for small gauge pars plana vitrectomy and peeling of the internal limiting membrane in naïve diabetic macular edema: The VITAL Study. *PLoS One* 2018;13(7):e0200365.
21. Kumagai K, Hangai M, Ogino N, et al. Effect of internal limiting membrane peeling on long-term visual outcomes for diabetic macular edema. *Retina* 2015;35(7):1422–1428.
22. Simunovic MP, Hunyor AP, Ho IV. Virectomy for diabetic macular edema: a systematic review and meta-analysis. *Can J Ophthalmol* 2014;49(2):188–195.
23. Ichiyama Y, Sawada O, Mori T, Fujikawa M, Kawamura H, Ohji M. The effectiveness of vitrectomy for diffuse diabetic macular edema may depend on its preoperative optical coherence tomography pattern. *Graefes Arch Clin Exp Ophthalmol* 2016;254(8):1545–1551.
24. Otani T, Kishi S, Maruyama Y. Patterns of diabetic macular edema with optical coherence tomography. *Am J Ophthalmol* 1999;127(6):688–693.
25. Seo KH, Yu SY, Kim M, et al. Visual and morphological outcomes of intravitreal ranibizumab for diabetic macular edema based on optical coherence tomography patterns. *Retina* 2016;36(3):588–595.
26. Shimura M, Yasuda K, Nakazawa T, et al. Visual outcome after intravitreal triamcinolone acetonide depends on optical coherence tomographic patterns in patients with diffuse diabetic macular edema. *Retina* 2011;31(4):748–754.
27. Shimura M, Yasuda K, Yasuda M, et al. Visual outcome after intravitreal bevacizumab depends on optical coherence tomographic patterns in patients with diffuse diabetic macular edema. *Retina* 2013;33(4):740–747.
28. Foos RY, Kreiger AE, Forsythe AB, et al. Posterior vitreous detachment in diabetic subjects. *Ophthalmology* 1980;87(2): 122–128.
29. Sebag J, Buckingham B, Charles MA, et al. Biochemical abnormalities in vitreous of humans with proliferative diabetic retinopathy. *Arch Ophthalmol* 1992;110(10):1472–1476.
30. Ziada J, Hagenau F, Compera D, et al. Vitrectomy for intermediate age-related macular degeneration associated with tangential vitreomacular traction: a clinicopathologic correlation. *Retina* 2018;38(3):531–540.
31. Visse R, Nagase H. Matrix metalloproteinases and tissue inhibitors of metalloproteinases: structure, function, and biochemistry. *Circ Res* 2003;92(8):827–839.
32. Abu El-Asrar AM, Mohammad G, Nawaz MI, et al. Relationship between vitreous levels of matrix metalloproteinases and vascular endothelial growth factor in proliferative diabetic retinopathy. *PLoS One* 2013;8(12):e85857.
33. Kowluru RA, Zhong Q, Santos JM. Matrix metalloproteinases in diabetic retinopathy: potential role of MMP-9. *Expert Opin Investig Drugs* 2012;21(6):797–805.
34. Lee S, Jilani SM, Nikolova GV, et al. Processing of VEGF-A by matrix metalloproteinases regulates bioavailability and vascular patterning in tumors. *J Cell Biol* 2005;169(4):681–691.
35. Sakamoto T, Ishibashi T. Hyalocytes: essential cells of the vitreous cavity in vitreoretinal pathophysiology. *Retina* 2011;31:222–228.

36. Lazarus HS, Hageman GS. In situ characterization of the human hyalocyte. *Arch Ophthalmol* 1994;112:1356–1362.
37. Schumann RG, Eibl KH, Zhao F, et al. Immunocytochemical and ultrastructural evidence of glial cells and hyalocytes in internal limiting membrane specimens of idiopathic macular holes. *Invest Ophthalmol Vis Sci* 2011; 52:7822–7834.
38. Zhao F, Gandorfer A, Haritoglou C, et al. Epiretinal cell proliferation in macular pucker and vitreomacular traction syndrome: analysis of flat-mounted internal limiting membrane specimens. *Retina* 2013;33:77–88.
39. Hata Y, Sassa Y, Kita T, et al. Vascular endothelial growth factor expression by hyalocytes abd ist regulation by glucocorticoid. *Br J Ophthalmol* 2008;92:1540–1544.
40. Lee SS, Ghosn C, Yu Z, et al. Vitreous VEGF clearance is increased after vitrectomy. *Invest Ophthalmol Vis Sci* 2010; 51(4):2135–2138.
41. Koyanagi Y, Yoshida S, Kobayashi J, et al. Comparision of effectiveness of intravitreal ranibizumab for diabetic macular edema in vitrectomized and nonvitrectomized eyes. *Ophthalmologica* 2016;236(2):67–73.
42. Kumagai K, Furukawa M, Ogino N, et al. Long-term follow-up of vitrectomy for diffuse non-tractional diabetic macular edema. *Retina* 2009;29:464–472.
43. Yamada Y, Suzuma K, Ryu M, et al. Systemic factors influence the prognosis of diabetic macular edema after pars plana vitrectomy with internal limiting membrane peeling. *Curr Eye Res* 2013;38(12):1261–1265.